

ABUNDANCES FROM $z=0$ TO $z=5$

DONALD G. YORK

*The University of Chicago
Department of Astronomy & Astrophysics
5640 S. Ellis Avenue
Chicago, IL 60637
USA*

Abstract.

Interstellar abundances are compared for the Milky Way disk, the Milky Way halo, the Large and Small Magellanic Clouds and the damped Lyman alpha systems among the QSO absorption line systems. While a new set of observational aspects of element formation in the Universe is emerging, including a dearth of formation activity from $z=5$ to $z=3$, the predicted signal of $[\text{Si}/\text{Fe}]$ decreasing from high z to low z , as Type I supernovae start contributing to Fe production, has not yet been seen.

1. Background

New telescopes and spectrographs now permit the study of the abundances of most of the first 30 elements in the periodic table in the interstellar gas. Following the determination of the first accurate abundances in gas clouds in the vicinity of the Sun, using the *Copernicus* telescope and spectrograph[(1)], modest resolution spectra of QSO absorption lines (QSOALS, the same resonance lines used in *Copernicus* studies, but redshifted into the 3500-9000 Å region) were used to compare abundances for intergalactic gas clouds with those found in local Milky Way gas[(2)]. Observations with the *Hubble Space Telescope* allowed improvement and extensions of the former studies[(3)]. Observations with 4 meter telescopes[(4)(5),(6)] and, more recently, the Keck telescope[(7),(8)], have dramatically improved our understanding of abundances in the absorbers with $z_{\text{abs}} < z_{\text{em}}$ in spectra of QSOs.

I summarize here observations of local clouds, gas in the Small and Large Magellanic Clouds, and results from QSOALS from $z=0.5$ to 5. Particular emphasis is given to abundances of those species that, by virtue of column density, intrinsic line strengths, ionization properties and line placement, can be determined over a wide range of redshifts, of z , namely C, Si, Fe and Zn. For intercomparing gas at different z , it is convenient to measure abundances relative to zinc, referenced to solar relative abundances of the same elements. The relation $[X/Y]$ refers to ratios by number of species X and Y (dex.) The notation $[X/Y]_{\odot}$ refers to the abundance referenced to the Sun.

2. The Galaxy

Steady improvements have occurred in our knowledge of abundances in local clouds. The improvements stem from better instruments and from improved knowledge of oscillator strengths (f -values.) In particular, for N° , O° , Si^{+} , Fe^{+} and Ni^{+} there exist lines weak enough to be unsaturated in local clouds with neutral hydrogen column densities $N(H\ I) < 10^{21}\text{ cm}^{-2}$. As has been known with low precision for some time, a pattern of depletion compared to solar abundances is seen in interstellar gas clouds which can be identified with three types of gas: cold clouds (ζ Oph B [(9)], warm clouds (i.e. ζ Oph A [(9)], α Vir [(10)]), and halo clouds [(11)]. The most extreme depletions, interpreted as showing species of low gas density due to condensation on dust grains, occur in cold clouds[(12)] (Figure 1). The same pattern, but with successively less extreme depletion, !! occurs in warm clouds and in halo clouds. The depletions for the three types of gas and for selected elements are shown as solid lines in Figure 2[(13)].

Note that the depletions shown are with reference to Zn. This presentation is chosen because the abundances of high precision are based on column densities of first ions, the dominant stage of ionization for the species shown in an interstellar radiation field. Both H I and H II regions are represented in these measurements. Thus, a direct comparison with H is not possible as only $N(H\ I)$ could be determined from absorption line observations. A literature search [(13)] reveals the errors in the ratios chosen here, owing to the different ionization potentials and to different local radiation fields, are less than ± 0.2 . The log of the ratio $N(Zn\ II)/N(H\ I)$ is shown at the far right. For regions represented here by the mean depletions shown, H I dominates over H II, but the relative amounts of H I and H II are unknown in detail.

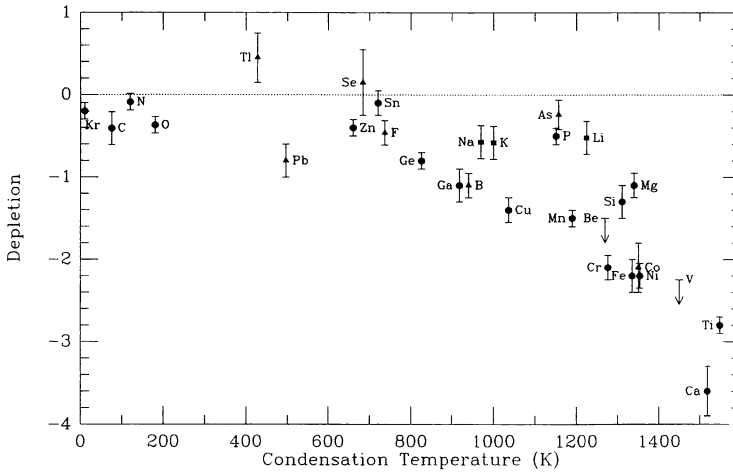


Figure 1. The variation of interstellar depletion for 30 elements with condensation temperature for an average dense cloud.

3. The Large and Small Magellanic Clouds

Depletions were determined for groups of lines (typically 4 - 5 components in 10 km^s⁻¹ wide complexes) toward Sk 108 in the SMC[(13)] and toward SN 1987A in the LMC[(14)]. Various means were used to show that, in all likelihood, H I regions are mainly represented by these depletions, though H II, in lesser quantities, exists alongside the H I, so much so that N II emission used in studying light echoes[(15)] can be correlated with the velocities of the absorption lines.

The results are shown by labelled symbols in Figure 2. The values are average depletions over five complexes toward Sk 108 and over eight complexes toward SN 1987A. No cold cloud pattern is formed toward SN 1987A, though narrow K I lines from gas with T ≤ 300 °K were observed with the AAT[(5)]. Either the column densities of dominant ions from the cold regions are much less than those from warm and halo clouds, or cold clouds in the LMC are depleted only as much as warm clouds in the Galaxy. This situation should be soon clarified by observation of the H₂ in the SMC and the LMC with the *FUSE* satellite. At any rate, the warm cloud and the halo cloud depletion pattern dominate LMC gas toward SN 1987A.

For Sk 108, only the halo cloud depletion pattern is seen: abundances, relative to Zn, of all elements studied are within 0.5 dex of solar.

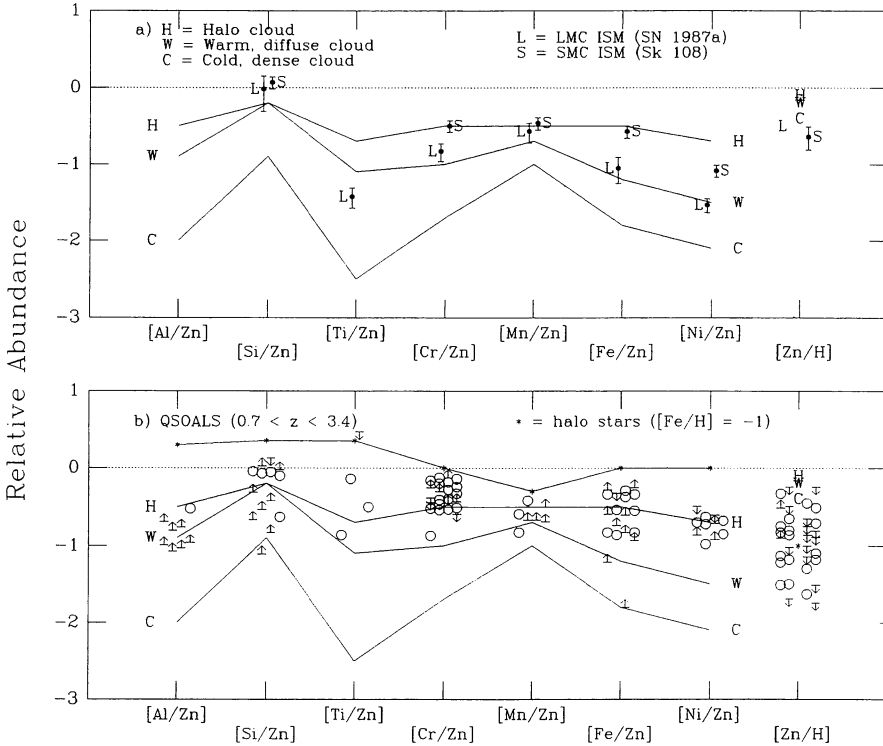


Figure 2. Average abundances (solid or open circles) for systems of interstellar lines in the LMC/SMC (top) or QSO absorption lines (bottom). Solid lines connect mean abundances for three distinct types of interstellar clouds. Abundances are referenced to zinc (Zn II) to minimize ionization corrections for the first ions observed for the other elements shown. At the right is an indicator of total metallicity $[Zn/H]$ based on $[ZnII/HI] - [Zn/H]_{\odot}$.

4. QSO Absorption Lines

4.1. DAMPED LYMAN ALPHA SYSTEMS

Some 40 damped Lyman alpha clouds have now been studied [(7), (8)]. Data summarized in references [(7) and [(8)] are shown in Figure 2 averaged over all systems. Zn II is not generally detectable at the highest redshifts, explaining the upper limits at the highest redshifts. However, in halo type clouds (depletion wise), Si is essentially undepleted compared to Zn. Where both Si and Fe are observed, the trends are the same as for the averages in Figure 2.

Note again the values $[Zn/H]$ at the far right. The absolute abundances of Zn consistently decrease with increasing z . The values of $[Fe/H]$ in cold clouds in the Milky Way are similar to those in QSOALS, evidently be-

cause solar abundance local gas has depleted Fe into grains ($[\text{Fe}/\text{H}] \sim 0.001$ $[\text{Fe}/\text{H}]_o$) whereas in many QSOALS, gas little depleted on grains has simply not reached solar abundance yet.

In the case of the QSOALS, it is not clear that the abundances are anything more than upper limits. Observations of Si II and O I in a few systems[(4),(16)] suggest that $[\text{O I}/\text{H I}]$ referenced to $[\text{O}/\text{H}]_o$ is lower than $[\text{Si II}/\text{H I}]$ referenced to $[\text{Si}/\text{H}]_o$. Assuming O and Si track each other owing to similar origins in type II SNe, the observations suggest that H II regions dominate over H I regions. (O I and H I track each other in ionization, so O I is largely destroyed in H II regions, whereas Si II remains a dominant ionization stage.) The alternative is that in the earliest SNe, Si is generated in greater masses relative to O in the ejecta than is the case at later times.

4.2. THE LYMAN ALPHA FOREST

Indications that there is a forest of C IV and Si IV doublets corresponding to the forest of Lyman alpha lines[(17)] and that $[\text{Si}/\text{C}]$ is higher in these systems than in the local interstellar medium [(18)] have recently been confirmed [(19)] by extension to systems with $N(\text{H I}) \geq 10^{15} \text{ cm}^{-2}$ and $[N(\text{H II})/N(\text{H I})] > 10^3$. The observations extend to $z = 4.5$, higher than the observations of damped Lyman alpha systems. Coupled with models of the ionization field from QSO radiation [(19),(20)], the data indicate a floor to heavy element abundances to the redshift limit so far observed [(21)].

5. Discussion

Gas phase abundance determinations indicate that heavy elements existed in QSOALS as early as $z = 5$, though at low levels. However, a marked increase in metallicity is noted beginning at $z = 3$. The results are consistent with an early universal contamination of primordial gas by massive stars, a delay in forming additional heavy elements until $z \sim 3$ [(22)] and a rise to 0.1 of solar abundances by $z = 2$. The abundances of Ca and Fe as seen in QSOALS do not show a further increase at $z < 1$ [(23)] to fully solar values, presumably because the disks analogous to the Milky Way in which solar abundance stars exist provide such a small cross section for absorption against background quasars, compared to the antecedent dwarf galaxies [(24)(25)] that may dominate at $z > 1$. Of course, as warm and cold cloud depletion patterns appear in low z galaxies, by analogy with the local interstellar medium, Ca, Fe and Si will be depleted, another possible explanation for the lack of solar abundances in low z QSOALS. As the poorly observed category of QSOALS from $z = 0$ to 1 is pursued [(6),(25)], more solar abundance systems should be seen in the species sulfur, zinc, oxygen and nitrogen (elements unaffected by depletion onto dust).

The data above should challenge and inform theoretical studies of nucleosynthesis as a function of time. For instance, the common observation of $[\text{Si}/\text{Zn}] \sim [\text{Si}/\text{Zn}]_0$ at high z , at times before SNe Ia could probably occur, suggests that Zn is a product of type II SNe [(26)], and not predominately associated with Type I SNe as some authors assume. The ratios $[\text{Si}/\text{C}]$ above $z = 3$ should aid in determining the mass of the first stars. The appearance of SNe at later times from successively less massive progenitors may be reflected in ratios $[\text{O}/\text{Si}]$ in gas phase as a function of z with implications for the stellar mass function between $z = 1$ and $z = 3$. Further observations of Mn and Cu (odd-even nuclei) may show a measurable increase in ratios such as Mn/Fe and Cu/Fe as z increases [(27)]. Increased sample size may allow detection of the decrease in $[\alpha/\text{Fe}]$ (abundance of C, O, Si and other type II products compared to iron) with decreasing redshift. The excess is hinted at by comparison of $[\text{Fe}/\text{Si}]$ in QSOALS (Fig. 2), but that result could be caused by residual dust depletion of Fe, in light of the fact that $[\text{Si}/\text{Zn}]$ found in QSOALS is not seen to reach the value 0.4 found in old halo stars in the Milky Way [(28)].

I am indebted to my colleagues Priscilla Frisch, Richard Green, Lew Hobbs, Varsha Kulkarni, Jim Lauroesch, Dave Meyer, Jim Truran and Dan Welty whose shared verbal contributions equal the contributions noted in the references. David Achenbach and Chris Mallouris helped in the preparation of the paper.

References

1. Rogerson, J. B., Spitzer, L., Drake, J. F., Dressler, K., Jenkins, E. B., Morton, D. C., and York, D. G. 1973, *ApJ*, **181**, L97
2. Smith, H. E., Jura, M. and Margon, B. 1979, *ApJ*, **228**, 369
3. Savage, B. D. and Sembach, K. R. 1996, *ARA&A*, **34**, 279
4. Kulkarni, V. P., Huang, K. L., Green, R. F., Bechtold, J., Welty, D. E., and York, D. G. 1996, *MNRAS*, **279**, 197
5. Pettini, M., Smith, L. J., Hunstead, R. W. and King, D. L. 1994, *ApJ*, **426**, 79
6. Robertson, J., Morton, D. C., Blades, J. C., York, D. G. and Meyer, D. M. 1988, *ApJ*, **325**, 635
7. Lu, L., Sargent, W. L. W., Barlow, T. A., Churchill, C. W. and Vogt, S. S. 1996, *ApJ*, **107**, 475
8. Prochaska, J. X. and Wolfe, A. M. 1997, *ApJ*, **474**, 140
9. Sofia, U. J., Cardelli, J. A. and Savage, B. D. 1994, *ApJ*, **430**, 650
10. York, D. G. and Kinahan, B. F. 1979, *ApJ*, **228**, 127
11. Spitzer, L. and Fitzpatrick, E. L. 1995, *ApJ*, **445**, 196
12. Hobbs, L. M., Welty, D. E., Morton, D. C., Spitzer, L. and York, D. G. 1993, *ApJ*, **411**, 750
13. Welty, D. E., Lauroesch, J. T., Baldes, J. C., Hobbs, L. M. and York, D. G. 1997, *ApJ*, **489**, 672
14. Welty, D. E., Frisch, P. C., Sonneborn, G. and York, D. G. 1999, *ApJ*, in press
15. Xu, J., Crotts, A. P. S., and Kunkel, W. E. 1995, *ApJ*, **451**, 806
16. Lauroesch, J. T., Truran, J. W., Welty, D. E. and York, D. G. 1996, *PASP*, **108**, 641
17. Meyer, D. M. and York, D. G. 1987, *ApJ*, **315**, L5

18. Khare, P., York, D. G. and Green, R. 1989, *ApJ*, **347**, 627
19. Cowie, L. L., Songaila, A., Kim, T. and Hu, E. M. 1995, *AJ*, **109**, 1522
20. Meiksin, A. and Madau, P. 1993, *ApJ*, **412**, 34
21. Songaila, A. 1997, *ApJ*, **490**, L1
22. Timmes, F. X., Lauroesch, J. T. and Truran, J. W.. 1995, *ApJ*, **451**, 468
23. Meyer, D. M. and York, D. G. 1992, *ApJ*, **399**, L121
24. York, D. G., Dopita, M., Green, R. and Bechtold, J. 1986, *ApJ*, **311**, 610
25. Ellis, R. 1999, *Nature*, xxx, xxx. (Astroph9807287).
26. Timmes, F. X., Truran, J. W., Lauroesch, J. T. and York, D. G. 1997, *ApJ*, **476**, 464
27. Truran, J. W. & Cameron, A. 1971, *ApJS*, **14**, 179
28. Wheeler, J. C., Sneden, C. and Truran, J. W. 1989, *ARA&A*, **27**, 279